Journal of Solid Mechanics Vol. 5, No. 1 (2013) pp. 47-62

An Efficient C_0 Finite Element Approach for Bending Analysis of Functionally Graded Ceramic-Metal Skew Shell Panels

G. Taj*, A. Chakrabarti

Department of Civil Engineering, Indian Institute of Technology, Roorkee-247 667, India

Received 26 January 2013; accepted 19 March 2013

ABSTRACT

In this article, the prominence has been given to study the influence of skew angle on bending response of functionally graded material shell panels under thermo-mechanical environment. Derivation of governing equations is based on the Reddy's higher-order shear deformation theory and Sander's kinematic equations. To circumvent the problem of C_1 continuity requirement coupled with the finite element implementation, C_0 formulation is developed. A nine noded isoparametric Lagrangian element has been employed to mesh the proposed shell element in the framework of finite element method. Bending response of functionally graded shell under thermal field is accomplished by exploiting temperature dependent properties of the constituents. Arbitrary distribution of the elastic properties follows linear distribution law which is a function of the volume fraction of ingredients. Different combinations of ceramic-metal phases are adopted to perform the numerical part. Different types of shells (cylindrical, spherical, hyperbolic paraboloid and hypar) and shell geometries are concerned to engender new-fangled results. Last of all, the influence of various parameters such as thickness ratio, boundary condition, volume fraction index and skew angle on the bending response of FGM skew shell is spotlighted. Some new results pertain to functionally graded skew shells are reported for the first time, which may locate milestone in future in the vicinity of functionally graded skew shells.

Keywords: Functionally graded material; Skew shell; Higher order shear deformation theory; Bending analysis; Thermal field

1 INTRODUCTION

THE supremacy of functionally graded materials (FGMs) over homogenous conventional materials and the ability to fabricate the material with graded properties in the favored direction made them to occupy fore-font in the material research. In general, FGMs are made by two isotropic constituents to propose two distinct properties: the first phase which is engineering metal may have alloys such as aluminium, titanium and steel and the other phase being ceramic comprise of alumina, zirconia and silicon carbide. The user can opt for appropriate blend of these two materials to realize the merits offered by each constituent. Owing to the potential to withstand ultra high temperature and large temperature changes that occurs with in a fraction of seconds, FGMs are widely used in space shuttles, nuclear reactors, solar panels and aerospace structures. As a final observation concerning FGMs, it can be noted that these graded materials concept has demonstrated that compositional micro/macrostructure gradient can not only dismiss undesirable effects such as stress concentration, but can also generate unique positive function [1]. Recently, an in-depth assessment on static, vibration and buckling problems of FGM plates was lucratively given by Jha et al. [2]. In addition, the reader can locate inestimable literatures available in the past to understand the behavior of FGM

* Corresponding author. Tel.: +91 1332 285844 ; Fax: +91 1332 275568.
E-mail address: gulshantaj19@yahoo.co.in (G. Taj).

structures [3-16]. For the sake of shortness, here we concise our attention to recapitulate the works performed on analysis of isotropic and FGM shells that utilize shear deformation theories in conjunction with various analytical and numerical techniques.

Many classical theories were evolved based on Love's assumption to analyze the elastic laminated shells [17-19]. But these theories are proven to be substandard in case of thick shells, due to the negligence of transverse shear effect. Further, to overcome the drawbacks of the classical theories, transverse shear stresses are taken to care by many researchers [20-22]. In due course of time, many displacement based higher order theories were also developed [23, 24], but the major drawback was the assumption of constant variation of transverse shear stresses thus leading to the estimation of shear correction factor. To end with, a simple higher order theory that accounts for parabolic variation of transverse shear stresses was proposed by Reddy [25], to eradicate the shear correction factor. The theory is based on the displacement field in which the displacements of the middle surface are expanded as cubic function of thickness coordinate which is equivalent to neglecting the stretching effect of normal to the middle surface of the shell. In addition, Reddy and Arciniega [26] carried out a comprehensive study of various plate and shell theories available till now, for vibration, bending and buckling analysis of plates and shells. Despite of the above pointed out research works, a substantial number of literatures are also available based on meshless methods supplemented with radial basis collocation technique [27-31]. Over a period of time, the focus has been diverted to utilize these developed theories for the analysis of functionally graded structures. Furthermore, some of the imperative earlier works in the area of FGM shells which serves the channel for the present study has been discussed in this section.

Pradyumna et al. [32] carried out the transient analysis of FGM shell panels by considering parabolic distribution of transverse shear strains along the thickness of the shell. Element with nine degrees of freedom per each node is utilized to develop C_0 finite element formulation. Zhao and Liew [33] studied the response of FGM shell panels based on the non-linear Sander's shell theory and geometric non linearity is taken into account for the analysis. Mesh free kernel particle functions, are length method and Newton-Raphson methods are employed in the study. They pointed out that volume fraction index plays dominant role and there may be significant influence on stresses when the panel is under thermal field. Zhao et al. [34] presented the Sander's first order shear deformation shell theory and used mesh-free kernel particle functions to carry out the static and vibration analysis of functionally graded shells under thermal and mechanical loads. Naghdabadi and Kordkhejli [35] presented a finite element formulation based on explicit through the thickness integration scheme for the thermoelastic analysis of FGM plates and shells. Cinefra et al [36] analysed the simply supported FGM shell under thermal field and transverse mechanical loads. Unified formulation with single and layer wise theory is used to analyze the panel. A series of studies on vibration and stability of circular shells with ring support under different loading environment is performed by Najafizadeh et al. [37-42].

Subsequently, considerable amount of work has been also published in relative to the analysis of FGM shells [43-47] considering non linearity into account. However, as far as the author's knowledge is concern, immense works were placed in the literature on the subject of bending response of FGM plates, but still, there is scarceness of results for the bending analysis of FGM shell panels with skew boundary which has specific application in modern construction structures. Hence, the authors are provoked to put forward the bending analysis of functionally graded panels by incorporating C_0 finite element formulation to acquire the cause of skew boundary in FGM shells. The material properties are assumed to have a smooth and gradual variation along the thickness direction of the shell and obey linear distribution law. Both thin and thick shells have been analyzed and the influence of skew angle (α), thickness ratio (R/h), volume fraction index (n) and boundary conditions on deflection parameter of the shell are accomplished in the form of Tables and Figures.

The paper is structured in the following fashion. Section 1 serves as platform for the present paper while giving brief idea on earlier related research works. In order to give an unambiguous motivation of the present study, we first furnish the significance of the present work in view of research under Section 2 and shell geometry considered with the FGM material properties is presented next in Section 3. A kinematics equation that describes the proposed model along with the strain part is surrendered in Section 4. A brief remark on the output of the various numerical problems is highlighted in Section 5 followed by summary bulletin of the study under Section 6.

2 RESEARCH SIGNIFICANCE

Skew shells which have ample employment in diverse fields of engineering demand the thorough understanding of

response in bending under various loading conditions. Hitherto, there are no works in the scientific literature regarding the bending analysis of FGM skew shells incorporating mechanical and thermal field using finite element as a tool. This is the root cause why the authors are motivated to accomplish the bending analysis of functionally graded skew shell panels using an efficient displacement based finite element approach, which is considered to be a most versatile and consistent tool to handle problems involving more complexity. The displacement field proposed in the present study (refer Eq. (5)), involves the derivatives of the out-of-plane displacement in in-plane displacement field (*u* and *v*). Further, this would invite the problem what is known as C_1 continuity requirement by involving second order derivatives in the strain part. Picking C_1 continuity invites complication and involvedness which is well established one and C_0 continuity allows the easy execution of isoparametric finite element formulation. Owing to the fact, C_0 elements can be applied to non-rectangular plan forms such as skew shells without involving any intricacy. For this intention, in the present formulation the strain vector having only the first-order derivatives has been evolved, thereby leading to a C_0 formulation. The significance of the present work can be recapitulated as below.

- An efficient C_0 element is developed for the finite element implementation which matches with other elements in practical owing to its unproblematic sense.
- Novel results are generated considering skew angle as the prime variable to ascertain the bending analysis of FGM shells under thermo-mechanical environment.
- Hyperbolic parabolid and hypar type skew shells which are known for its special form of its geometry, and not yet considered in any of the earlier works are analyzed using third order shear deformation theory (TSDT).
- Special form of displacement field proposed by Reddy [48] is incorporated to accomplish strain-displacement relation, thus eliminating the use of shear correction factor which is the cumbersome process otherwise.

By presenting the various important conclusions regarding bending of functionally graded skew shell (FGSS) incorporating various parameters and shell types, the authors confident that, the presented results should serve as crucial reference data in case of FGM skew shells.

3 FUNCTIONALLY GRADED MATERIALS

3.1 Geometry of FGSS

A shell element having dimensioned *a* x *b* x *h* and skew angle α is represented in Cartesian co-ordinate system as demonstrated in Fig. 1. The mid plane of the shell (z=0) is assumed as reference plane for the material co-ordinate system. The top surface of the shell (z=+h/2) is rich in ceramic content, whereas the bottom surface of the shell (z=-h/2) is rich in metal content. The finite element implementation of the model is based on the application of the nine noded isoparametic Lagrangian element with seven nodal unknowns per node (Fig. 2).

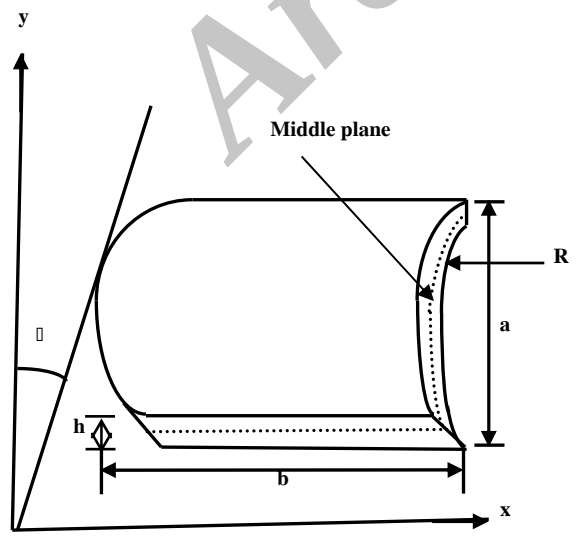

Fig. 1
Geometry of cylindrical skew shell.

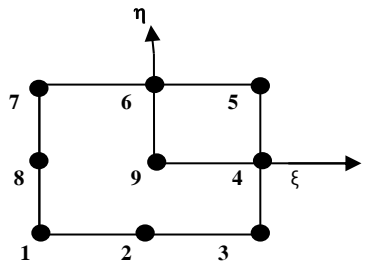

Fig. 2
Isoparametric Lagrangian element in natural co-ordinate system.

3.2 FGM properties

In common, FGMs are characterized by their smooth and gradual variation of material properties along the preferred direction. In the present study, the effective material properties of the shell panel are assumed to vary only in the thickness direction. Different schemes are proposed in the literature to evolve the effective properties of the functionally graded materials. Amid the methods projected in the literature: Self consistent scheme [49-51] Mori and Tanaka scheme [52, 53] composite sphere assemblage model [54, 55] composite cylindrical assemblage model [56, 57] simplified strength of materials method [58, 59] method of cells [60] and Voigt rule of mixture [61] are few to cite. Even though each scheme has its own pros, Voigt rule of mixture [61] dominate the literature and henceforth utilized in the study. As per Voigt method, the effective property (P) of FGSS can be expressed as:

$$P = P_c V_c + P_m V_m \tag{1}$$

where V_c and V_m are the volume fraction of the ceramic and metal phase of the FGM shell, respectively. In the present study, Eq. (1) is utilized to homogenize Young's modulus (E), Poisson's ratio (γ), thermal conductivity (k), thermal expansion (α) and density (ρ) of the material. The volume fraction of the ceramic part (V_c) can be estimated from the linear distribution law which can be expressed in its mathematical form as:

$$V_c = \left(\frac{z}{h} + 0.5\right)^n \tag{2}$$

It should be obvious that n is the non-negative parameter and referred in the literature by diverse terms as volume fraction index, power law index, power law exponent and power law constant. Here, we refer the constant n as volume fraction index in all the sections. It assumes the value between zero and infinity. The value of n=0 corresponds to top of the shell (z=+h/2) which is rich in ceramic content, and infinity corresponds to bottom of the shell (z=-h/2) which is rich in metal content. By varying the magnitude of n between zero and infinity, the user can predict the properties of the functionally graded material at any location (depth) in the simple manner. Further, the volume fraction of the ceramic and metal phases are correlated by the relation,

$$V_c + V_m = 1 \tag{3}$$

By assuming the plane stress condition (σ_{zz}=0), the linear constitutive relation for the FGM shell may be expressed as:

$$\begin{Bmatrix} \sigma_{xx} \\ \sigma_{yy} \\ \sigma_{yz} \\ \sigma_{xz} \\ \sigma_{xy} \end{Bmatrix} = \begin{bmatrix} Q_{11} & Q_{12} & 0 & 0 & 0 \\ Q_{21} & Q_{22} & 0 & 0 & 0 \\ 0 & 0 & Q_{33} & 0 & 0 \\ 0 & 0 & 0 & Q_{44} & 0 \\ 0 & 0 & 0 & 0 & Q_{55} \end{bmatrix} \left(\begin{Bmatrix} \varepsilon_{xx} \\ \varepsilon_{yy} \\ \gamma_{yz} \\ \gamma_{xz} \\ \gamma_{xy} \end{Bmatrix} - \begin{Bmatrix} 1 \\ 1 \\ 0 \\ 0 \\ 0 \end{Bmatrix} \alpha(z,T)\Delta T \right) \tag{4}$$

where $Q_{11}=Q_{22}=\frac{E(z)}{1-\gamma^2}$, $Q_{12}=Q_{21}=\frac{\gamma E(T)}{1-\gamma^2}$, $Q_{33}=Q_{44}=Q_{55}=\frac{E(z)}{2(1+\gamma)}$, Q_{ij} is the stiffness coefficient matrix depends on the Young's modulus (E) and Poisson's ratio (γ) of the material. Here, thermal expansion co-efficient (α) is a function of depth (z) and temperature (T) of the material.

4 FINITE ELEMENT FORMULATION

4.1 Kinematics

A special form of displacement field proposed by Reddy [48] is chosen, which can be dictated by the condition of zero transverse shear stresses ($\sigma_{xz}=\sigma_{yz}=0$) at the top and bottom and non-zero at any other location of the shell. The in-plane displacement field (u and v) presented here are expanded as cubic functions of the thickness coordinate (z), while the constant transverse displacement (w) through the thickness has been assumed. Any other choice of displacement field would either not satisfy the stress-free boundary conditions or lead to a theory that would involve more dependent unknowns than those in the first-order shear deformation theory [48]. The present finite element formulation is based on shallow shell theory and the middle plane of the shell is taken as the reference plane (see Fig.1). It is to be noted that, the theory given by Reddy assumes the parabolic variation of transverse shear stresses through the thickness of the shell, due to which the use of shear correction factor can be avoided. Meanwhile, the C^1 continuity requirement of the higher order theory has been circumvented in the present study by assuming the derivatives of the transverse displacement as separate field variables i.e., $\Psi_x^*=\left(\theta_x+\frac{\partial w}{\partial x}\right)$ and $\Psi_y^*=\left(\theta_y+\frac{\partial w}{\partial y}\right)$.

According to Reddy's third order shear deformation theory, the in-plane displacement field u and v and the transverse displacement w of the shell surface can be expressed as:

$$\begin{aligned} u &= u_0 + z\,\theta_x\left(1-\frac{4z^2}{3h^2}\right)-\frac{4z^3}{3h^2}\psi_x^* \\ v &= v_0 + z\,\theta_y\left(1-\frac{4z^2}{3h^2}\right)-\frac{4z^3}{3h^2}\psi_y^* \\ w &= w_0 \end{aligned} \tag{5}$$

Also, the displacement field at any point within the element can be written in-terms of nodal unknowns by using interpolation functions otherwise known as shape functions as:

$$\begin{aligned} &u=\sum_{i=1}^{9}N_i u_i \quad , \quad v=\sum_{i=1}^{9}N_i v_i \quad , \quad w=\sum_{i=1}^{9}N_i w_i \quad , \quad \theta_x=\sum_{i=1}^{9}N_i\theta_{xi} \quad , \quad \theta_y=\sum_{i=1}^{9}N_i\theta_{yi} \quad , \\ &\psi_x^*=\sum_{i=1}^{9}N_i\psi_{xi}^* \quad , \quad \psi_y^*=\sum_{i=1}^{9}N_i\psi_{yi}^* \end{aligned} \tag{6}$$

To define the deformation profile, the basic field variables interpreted in the present study are u_0, v_0, w_0, θ_x, θ_y, , , ψ_x^* and ψ_y^* for each node and hence a total number of 63 field variables are taken for the analysis of each element. In the present study, following shape functions are considered.

$$\begin{aligned} &N_1=\frac{1}{4}(\zeta-1)(\eta-1)\xi\eta \ , \ N_2=\frac{1}{4}(\xi+1)(\eta-1)\xi\eta \ , \ N_3=\frac{1}{4}(\xi+1)(\eta+1)\xi\eta \ , \\ &N_4=\frac{1}{4}(\zeta-1)(\eta+1)\xi\eta \ , \ N_5=-\frac{1}{2}(1-\zeta^2)(1-\eta)\eta \ , \ N_6=-\frac{1}{2}(1+\zeta)(\eta^2-1)\xi \ , \\ &N_7=-\frac{1}{2}(\zeta^2-1)(1+\eta)\eta \ , \ N_8=-\frac{1}{2}(\zeta-1)(\eta^2-1)\zeta \ , \ N_9=(1-\zeta^2)(1-\eta^2) \end{aligned} \tag{7}$$

4.2 Strain-Displacement relation

All the formulations are confined to linear elastic behavior with small displacements and small strains. The linear strain- displacement relations according to Sander's shell theory are

$$\begin{aligned}
\varepsilon_x &= \frac{\partial u}{\partial x} + \frac{w}{R_x} \\
\varepsilon_y &= \frac{\partial v}{\partial y} + \frac{w}{R_y} \\
\gamma_{xy} &= \frac{\partial u}{\partial y} + \frac{\partial v}{\partial x} + \frac{2w}{R_{xy}} \\
\gamma_{xz} &= \frac{\partial u}{\partial z} + \frac{\partial w}{\partial x} + \frac{C_1 u}{R_x} - \frac{C_1 v}{R_{xy}} \\
\gamma_{yz} &= \frac{\partial v}{\partial z} + \frac{\partial w}{\partial y} + \frac{C_1 v}{R_x} - \frac{C_1 u}{R_{xy}}
\end{aligned} \tag{8}$$

R_x, R_y represents the radii of curvature in the x and y directions respectively and R_{xy} is the twist radii of curvature. C_1 is the tracer that helps to reduce the approximation in to Love's shell theory and it is taken as unity in the present formulation. It is worth here to mention that, in Eq. (8), the term for twist radii of curvature (R_{xy}) will facilitate the formulation to handle shell with special geometry (i.e., hypar).Upon substitution of Eq. (5) in to Eq. (8), we get the strain terms as:

$$\begin{aligned}
\varepsilon_x &= \varepsilon_{x0} + z(1 - \frac{4z^2}{3h^2})k_x - \frac{4z^3}{3h^2}k_x^* \\
\varepsilon_y &= \varepsilon_{y0} + z(1 - \frac{4z^2}{3h^2})k_y - \frac{4z^3}{3h^2}k_y^* \\
\gamma_{xy} &= \gamma_{xy0} + z(1 - \frac{4z^2}{3h^2})k_{xy} - \frac{4z^3}{3h^2}k_{xy}^* \\
\gamma_{yz} &= \phi_y + z(1 - \frac{4z^2}{3h^2})k_{yz} - \frac{4z^3}{3h^2}k_{yz}^* - \frac{4z^2}{h^2}k_{yz}^{**} \\
\gamma_{xz} &= \phi_x + z(1 - \frac{4z^2}{3h^2})k_{xz} - \frac{4z^3}{3h^2}k_{xz}^* - \frac{4z^2}{h^2}k_{xz}^{**}
\end{aligned} \tag{9}$$

where

$$\left\{\varepsilon_{x0}, \varepsilon_{y0}, \gamma_{xy0}\right\} = \left\{\frac{\partial u_0}{\partial x} + \frac{w_0}{R_x}, \frac{\partial v_0}{\partial y} + \frac{w_0}{R_y}, \frac{\partial u_0}{\partial y} + \frac{\partial v_0}{\partial x} + \frac{2w_0}{R_{xy}}\right\}$$

$$\left\{\phi_x, \phi_y\right\} = \left\{\frac{\partial u}{\partial z} + \frac{\partial w}{\partial x} - \frac{C_1 u}{R_x} \frac{C_1 v}{R_{xy}}, \frac{\partial w}{\partial y} + \theta_y \frac{C_1 v_0}{R_x} \frac{C_1 u_0}{R_{xy}}\right\}$$

$$\left\{k_x, k_y, k_{xy}, k_x^*, k_y^*, k_{xy}^*\right\} = \left\{\frac{\partial \theta_x}{\partial x}, \frac{\partial \theta_y}{\partial y}, \frac{\partial \theta_x}{\partial y} + \frac{\partial \theta_y}{\partial x}, \frac{\partial \psi_x^*}{\partial x}, \frac{\partial \psi_y^*}{\partial y}, \frac{\partial \psi_x^*}{\partial y} + \frac{\partial \psi_y^*}{\partial x}\right\}$$

$$\left\{k_{xz}, k_{yz}, , k_{xz}^*, k_{yz}^*, k_{xz}^{**}, k_{yz}^{**}\right\} = \left\{-C_1 \frac{\theta_x}{R_x} - C_1 \frac{\theta_y}{R_{xv}} - C_1 \frac{\theta_y}{R_y} - C_1 \frac{\theta_x}{R_{xy}}, -C_1 \frac{\psi_x^*}{R_x} - C_1 \frac{\psi_y^*}{R_{xy}}, -C_1 \frac{\psi_y^*}{R_y} - C_1 \frac{\psi_x^*}{R_{xy}}, \theta_x + \psi_y\right.$$

Further, the strain matrix will involve the shape functions (N_i), derivatives of shape functions $\frac{\partial N_i}{\partial x}$ or $\frac{\partial N_i}{\partial y}$ and curvature terms (R_x, R_y and R_{xy}) as derived in Appendix A.

Hence, the strain vector in terms of displacement of each node may be expressed as:

$$\{\varepsilon\} = [B]\{\delta\} \tag{10}$$

In Eq. (10), [***B***] is the strain-displacement matrix and $\{\delta\}$ is the vector contains the nodal-displacement variables. where $\{\varepsilon\} = \{\varepsilon_{x0}, \varepsilon_{y0}, \gamma_{xy0}, \phi_x, \phi_y, k_x, k_x^*, k_y, k_y^*, k_{xy}, k_{xy}^*, k_{xz}, k_{xz}^*, k_{yz}, k_{yz}^*, k_{xz}^{**}, k_{yz}^{**}\}^T$

4.3 Governing equations

According to the principle of virtual, work the element stiffness matrix [***K***] and the load vector {***P***} can be derived as:

$$[K]_e = \int_{-1}^{+1}\int_{-1}^{+1} [B]^T [D][B]|J|\, d\xi d\eta \tag{11}$$

$$\{P\}_e = \int_{-1}^{+!}\int_{-1}^{+1} q[N]^T |J|\, d\xi d\eta \tag{12}$$

[**D**], [**J**] are the rigidity matrix and Jacobian matrix respectively, for the element under the consideration. The above formed stiffness matrix $[\boldsymbol{K}]_e$ and the load vector $\{\boldsymbol{P}\}_e$ at element level are assembled using the standard assembly procedure to get stiffness matrix and load vector at global level. The boundary conditions are imposed to get the nodal displacements and stresses are calculated using Eq. (4). Different types of boundary conditions are incorporated to study its response on the deflection parameter. A numerical code in FORTRAN 90 is developed to implement the above finite element formulation for the calculation of deflection in FGSS. The global stiffness matrix is stored in singly array using skyline method and Gaussian elimination procedure is used for the solution of simultaneous equations.

4.4 Boundary conditions

Following types of boundary conditions have been utilized to perform the various numerical problems. For the sake of brevity only the short term notations mentioned in the bracket are utilized wherever necessary.

Simply supported (SSSS):

$$u = w = \theta_v = \psi_v^* = 0 \ \ at \ x = 0, a$$
$$v = w = \theta_x = \psi_x^* = 0 \ \ at \ y = 0, b$$

Clamped (CCCC):

$$u = v = w = \theta_x = \theta_v = \psi_v^* = \psi_x^* = 0 \ \ at \ x = 0, a \ \ and \ \ y = 0,$$

Simply supported-clamped (SCSC):

$$u = w = \theta_v = \psi_v^* = 0 \ \ at \ x = 0, a$$
$$u = v = w = \theta_x = \theta_v = \psi_v^* = \psi_x^* = 0 \ \ at \ y = 0, b$$

Clamped-free (CFCF):

$$u = v = w = \theta_x = \theta_y = \psi_y^* = \psi_x^* = 0 \ \ at \ x = 0, a$$
$$u = v = w = \theta_x = \theta_y = \psi_y^* = \psi_x^* \neq 0 \ \ at \ y = 0, b$$

5 COMMENTS ON NUMERICAL STUDIES

To explain, this section is broken down into two major phases. In the first phase, to make certain the exactness and efficacy of the present formulation, the result obtained by the present higher order theory is compared with that of results presented by Zhao et al. [34] which utilizes the first order shear deformation theory (FSDT) and ensure the linear variation of shear strain through the thickness of the shell. In addition, the convergence study is also performed by taking different mesh sizes before proceeding to attain generate new results. In the second phase, an effort has been made by the authors to engender innovative results with respect to bending performance of FGM skew shell panels. However, the prime emphasis has been given to highlight the effect of skew angle on bending response of FGSS. The properties of the constituents of the material like Young's modulus (E), Poisson's ratio (γ), thermal conductivity (k), co-efficient of thermal expansion (α) and density (ρ) that depends on temperature has also been considered for thermal analysis. Following are the different properties of ceramic and metal constituents employed to perform the numerical part.

$$\text{Silicon Nitride } \left(Si_3N_4\right): \ E = \ 322.27GPa, \ \gamma = 0.24 \tag{13}$$

$$\text{Stainless Steel } \left(SUS_30_4\right): \ E = 207.78GPa, \ \gamma = 0.318 \tag{14}$$

$$\text{Aluminium } \left(Al\right): \ E = 70 \ GPa, \ \gamma = 0.3 \tag{15}$$

$$\text{Zirconia } \left(Zr0_2\right): \ E = 151 \ GPa, \ \gamma = 0.3 \tag{16}$$

$$\text{Alumina } \left(Al_20_3\right): \ E = 320.2 \ GPa, \ \gamma = 0.26 \tag{17}$$

The above mentioned ceramic and metal phases are combined together to carry out the validation study and generate new results. Three types of FGM shells: type I- $Al/Zr0_2$, type II- Al/Al_20_3 and type III SUS_30_4/Si_3N4 are considered. Unless otherwise specified, the dimensions of the shell panel used for all the examples are $a = b = 1$m, $R = 1$m, $h = 0.01$m. A mechanical load of magnitude $q = 1.0x10^6$ N/m^2 is applied in the transverse direction. All the results presented in the form of Tables and Figures are adimensionalized and different parameters handled in the study are represented below.

Displacement: $\bar{w} = \dfrac{w}{h}$

Axial stresses: $\bar{\sigma}_{xx} = \dfrac{\sigma_{xx} R^2}{q_0 h^2}$

5.1 Convergence and validation study

Table 1. enlightens the efficiency and convergence of the present formulation which compared with the source paper by Zhao et al. [34] based on first order shear deformation theory, using type I FGM cylindrical shell. An excellent agreement between the two papers is obvious. Based on the progressive mesh refinement, it is decided that 16x16 mesh is adequate for the bending analysis of FGM skew shells. Hence, in the present study a mesh of size 16x16 is adopted for all the numerical examples performed. For the sake of brevity, the mesh size is not mentioned in the subsequent Tables of the paper. Here, the volume fraction index n is chosen from 0 to 5. Different support conditions such as, simply supported-simply supported (SSSS), clamped-clamped (CCCC) and camped-simply supported (CSCS) are incorporated in the Table 1. The error percentage between the present and the source paper results are also exposed in Table 1. The least error is reported for the case of n= 0.5 related with simply supported condition and maximum error was noted to be around 2.27 with reference to n= 5.0 with clamped boundary condition. The discrepancy between the two results happens due to different theories involved to refer the kinematics field and the various solution strategies followed by the authors. It is to be noted that the different values of volume fraction index n have no pronounced influence on the convergence rate. Also, the shell with clamped-

clamped (CCCC) boundary undergoes less deflection followed by clamped-simply supported (CSCS) and simply supported (SSSS) boundaries. After ensuring the exactness of the present formulation, it is extended to engender new results by considering various shell types and geometry.

Table 1
Non dimensional central deflection of cylindrical shell (type I FGM)-convergence and validation

Boundary condition	Reference	Volume fraction index (n)					
		0	0.2	0.5	1	2	5
SSSS	Present (4x4)[a]	0.04235	0.04747	0.05367	0.06027	0.06612	0.07192
	Present (6x6) [a]	0.04265	0.04781	0.05405	0.06069	0.06657	0.07240
	Present (8x8) [a]	0.04272	0.04789	0.05414	0.06079	0.06668	0.07251
	Present (12x12) [a]	0.04275	0.04792	0.05419	0.06084	0.06673	0.07256
	Present (16x16) [a]	0.04275	0.04793	0.05419	0.06085	0.06674	0.07257
	Zhao et al. [34]	0.04267	0.04807	0.05425	0.06072	0.06658	0.07235
	% of error	0.19	0.29	0.11	0.21	0.24	0.30
CCCC	Present (16x16) [a]	0.01374	0.01539	0.01739	0.01953	0.02146	0.02341
	Zhao et al. [34]	0.01347	0.01516	0.01711	0.01915	0.02102	0.02289
	% of error	2.00	1.52	1.64	1.98	2.09	2.27
CSCS	Present (16x16) [a]	0.02161	0.02423	0.02740	0.03077	0.03375	0.03668
	Zhao et al. [34]	0.02122	0.02391	0.02700	0.03022	0.03310	0.03593
	% of error	1.84	1.34	1.48	1.82	1.96	2.09

[a] indicates mesh size.

5.2 New results-FGM skew shell
5.2.1 Skew cylindrical shell under mechanical load

In Table 2, an attempt has been made to study the influence of skew angle for type I FGM cylindrical shell (R_x=R, R_y=R_{xy}=∞) with several types of support condition. The considered value of skew angle ranges from 15° to 60° and several values of volume fraction index (n=0 to10) are also chosen. Three types of boundary conditions, simply supported-simply supported (SSSS), clamped-clamped (CCCC) and simply supported-clamped (SCSC) are adopted. It is noticed that hike in skew angle (α) tends to decline the deflection irrespective of the value of volume fraction (n) considered. Another important observation from the Table 2. , is that larger volume fraction (n) of the shell tends to boost up the deflection parameter. The low stiffness contributed by the metal segment of the shell may be the contribution factor for this type of tendency. Moreover, the shell with SSSS boundary condition endures the large amount of deflection than that of shell with CCCC and SCSC type of boundary condition. This is not surprising, because of the high rigidity phenomenon offered by clamped shell compared with other type boundary conditions. Further, the outcome regarding the effect of volume fraction index n on the deflection parameter remains unchanged as observed from Table 1. Finally, it can be interpreted that the volume fraction index n plays a key role in bending response of the plate.

5.2.2 Spherical, Hyperbolic paraboloid and hypar skew shells under mechanical load

In this problem, we assess the superiority of the shell type in bending by considering type-II FGM shell having different types of plan view. The other parameters considered in the problem remain same as mentioned in comparison part. Bending performance of three kinds of shell types namely spherical (R_x=R_y=R, R_{xy}=∞), hyperbolic paraboloid (R_x=-R_y) and hypar (R_x=R_y=∞) are demonstrated in Fig. 3. It is to be noted that the term R_{xy} incorporated in the strain part (refer Eq. (5)) will enable the formulation to handle the special form like hypar skew shells, which is the one of the major aspect of the present paper. The results are shown for the linear variation of ceramic and metal phase i.e, n=1.0. Four types of support conditions such as simply supported-simply supported (SSSS), clamped-clamped (CCCC), simply supported-clamped (SCSC) and clamped-free (CFCF) are evaluated. Among all the boundary conditions considered, clamped-free boundary condition (CFCF) endures the least bending response regardless of the shell type. Moreover, the hypar shells show better performance in comparison with spherical and hyperbolic paraboloid shell.

Table 2
Non dimensional central deflection of cylindrical skew shell (type I FGM)

Boundary condition	Skew Angle (α)	Volume fraction index (n)						
		0	0.2	0.5	1	2	5	10
SSSS	15°	0.04264	0.04792	0.05430	0.06096	0.06656	0.07184	0.07681
	30°	0.02993	0.03363	0.03810	0.04278	0.04672	0.05044	0.05393
	45°	0.01508	0.01694	0.01919	0.02155	0.02355	0.02546	0.02722
	60°	0.00440	0.00493	0.00559	0.00627	0.00687	0.00745	0.00797
CCCC	15°	0.01364	0.01531	0.01734	0.01947	0.02131	0.02310	0.02470
	30°	0.00943	0.01058	0.01198	0.01346	0.01474	0.01599	0.01710
	45°	0.00473	0.00531	0.00600	0.00674	0.00740	0.00805	0.00861
	60°	0.00145	0.00162	0.00183	0.00206	0.00227	0.00248	0.00266
SCSC	15°	0.02237	0.02513	0.02846	0.03196	0.03495	0.03781	0.04043
	30°	0.01558	0.01749	0.01981	0.02224	0.02434	0.02636	0.02819
	45°	0.00792	0.00888	0.01005	0.01129	0.01237	0.01343	0.01436
	60°	0.00245	0.00274	0.00310	0.00349	0.00383	0.00418	0.00447

5.2.3 Effect of radius and load parameter on displacement of skew cylindrical shell

Fig.4 exhibits the dominance of radius-thickness ratio over the deflection parameter of type II FGM, shell considering SSSS support condition. Three types of radius-thickness ratio R/h= 50, 100 and 200 are picked to study the effect of R_x on bending response of skew cylindrical shell. Several values of volume fraction index n=0.5, 1.0, 2.0 and 10 are utilized for the present example. The examination on Fig. 4 reads, as the radius tends to rise, stiffness of the shell becomes less there by reporting more deflection factor. Increase in volume fraction index corresponds to segment offers less stiffness and hence ensures maximum bending response. For the value of R/h=50 which means thickness h=0.02 shows almost least influence on the bending response of the plate is another output depicted from Fig.3. Further, for R/h=200 which means h=0.005 reflects drastic change in its behavior over other cases considered. The consequence of load parameter on non-dimensional deflection is exhibited in Fig.5 for several values of volume fraction index (n=0 to 1000). Increase in the load parameter confirms the rise in deflection parameter for all the values of volume fraction index considered. Further, the increase in volume fraction index n tends to lift the deflection, which is the same statement observed from previous examples also.

5.2.4 Skew cylindrical shell under thermal field

The consequence of temperature field on the bending response of the type-III FGM cylindrical shell is revealed in Table 4. The temperature dependent material properties of the constituents of the shell are displayed in Table 3 with relative units. Here, Young's modulus (E), Poisson's ratio (γ), thermal expansion co-efficient (a) thermal conductivity (k) and density (ρ) are taken as temperature-dependent properties under the temperature T=300K. The bottom temperature which refers to temperature of the metal segment is kept as unchanged (i.e., T_m=20°C), while the top temperature that corresponds to temperature of the ceramic segment takes the value from 100°C to 400°C. The repeating observation concluded from Table 2 with regard to skew angle is again confirmed in Table 4. (i.e., increase in skew angle lowers the deflection parameter).Further, amplification in temperature field be likely to rise the deflection regardless of the skew angle of the shell. This is because of the weak young's modulus of the material under high temperature.

5.2.5 Influence of axial stresses in skew cylindrical shell under mechanical load

Axial stresses of type II FGM cylindrical shell at the top and bottom surface of the shell panel subjected to transverse mechanical load was exhibited in Table 5. Effect of volume fraction index has been taken in to account by assuming several values of n=0, 1, 5 and 1000. It reveals the fact that bottom of the shell where z=-h/2 experiences the stresses which are compressive in character, while the top of the shell where z=+h/2 experiences the stresses which are tensile in character. Increase in skew angle tends the shell to have minimum stresses (either compressive or tensile in nature) at both top and bottom surfaces. Further, increase in volume fraction index n makes the shell to experience maximum stress (either compressive or tensile in nature).

Table 3
Temperature dependent properties of FGM constituents

Constituents	Elastic properties of FGM				
	E (x10^9N/m^2)	γ	α (x10^{-6}/^{0}C)	K (W/m-K)	ρ(kg/m^3)
Zirconia ($Zr0_2$)	151.0	0.30	23.0	204	2707
Aluminium (Al)	70.0	0.30	10.0	2.09	3000
Alumina (Al_20_3)	320.2	0.26	7.2	10.4	3750
SUS_30_4	207.78	0.318	15.3	9.54	8166
Si_3N_4	322.27	0.24	7.47	10.12	2370

Table 4
Effect of temperature field on non-dimensional deflection $\bar{w}$ of cylindrical skew shell (type III FGM, thermal load, T_{bottom}=20°C)

Skew angle (α)	T_{top}(°C)	Volume fraction index (n)					
		0	0.5	1	2	5	1000
15°	100	0.02030	0.01920	0.01940	0.02140	0.02730	0.04410
	150	0.03290	0.03120	0.03160	0.03480	0.04440	0.07170
	200	0.04560	0.04320	0.04370	0.04820	0.06140	0.09930
	250	0.05830	0.05510	0.05590	0.06150	0.07850	0.12700
	300	0.07100	0.06710	0.06800	0.07490	0.09550	0.15400
	350	0.08360	0.07910	0.08020	0.08830	0.11300	0.18200
	400	0.09630	0.09110	0.09230	0.10200	0.13000	0.21000
30°	100	0.01590	0.01510	0.01530	0.01680	0.02150	0.03470
	150	0.02590	0.02450	0.02480	0.02740	0.03490	0.05640
	200	0.03590	0.03390	0.03440	0.03790	0.04830	0.07810
	250	0.04580	0.04340	0.04390	0.04840	0.06170	0.09980
	300	0.05580	0.05280	0.05350	0.05890	0.07510	0.12200
	350	0.06580	0.06220	0.06310	0.06940	0.08860	0.14300
	400	0.07570	0.07170	0.07260	0.08000	0.10200	0.16500
45°	100	0.00998	0.00944	0.00957	0.01050	0.01340	0.02170
	150	0.01620	0.01530	0.01550	0.01710	0.02180	0.03530
	200	0.02250	0.02120	0.02150	0.02370	0.03020	0.04890
	250	0.02870	0.02710	0.02750	0.03030	0.03870	0.06250
	300	0.03490	0.03300	0.03350	0.03690	0.04710	0.07610
	350	0.04120	0.03890	0.03950	0.04350	0.05550	0.08970
	400	0.04740	0.04490	0.04540	0.05010	0.06390	0.10300
60°	100	0.00432	0.00408	0.00414	0.00456	0.00582	0.00942
	150	0.00701	0.00663	0.00672	0.00741	0.00946	0.01530
	200	0.00971	0.00919	0.00931	0.01030	0.01310	0.02120
	250	0.01240	0.01170	0.01190	0.01310	0.01670	0.02710
	300	0.01510	0.01430	0.01450	0.01600	0.02040	0.03300
	350	0.01780	0.01680	0.01710	0.01880	0.02400	0.03890
	400	0.02050	0.01940	0.01970	0.02170	0.02770	0.04480

Table 5
Non dimensional axial stresses for cylindrical shell (type II FGM, mechanical load)

Skew angle (α)	Volume fraction index (n)							
	0		1		5		1000	
	Top	Bottom	Top	Bottom	Top	Bottom	Top	Bottom
15°	0.1104e09	-0.79508e08	0.16848e09	-0.40741e08	0.23331e09	-0.62714e08	0.50517e08	-0.79508e08
30°	0.90266e08	-0.61881e08	0.13845e09	-0.31937e08	0.19182e09	-0.49126e08	0.41290e09	-0.61881e08
45°	0.60161e08	-0.40295e08	0.92840e08	-0.20950e08	0.12813e09	-0.32055e08	0.27519e09	-0.40295e08
60°	0.26999e08	-0.18978e08	0.41680e08	-0.98531e07	0.57312e08	-0.14996e08	0.12350e09	-0.18978e08

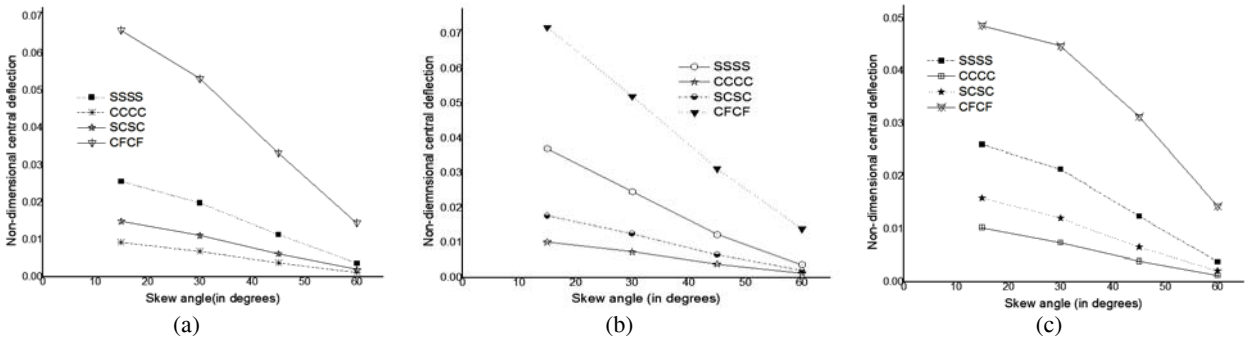

Fig. 3
Non dimensional central deflection of different shell types for various skew angles (type II FGM, mechanical load).

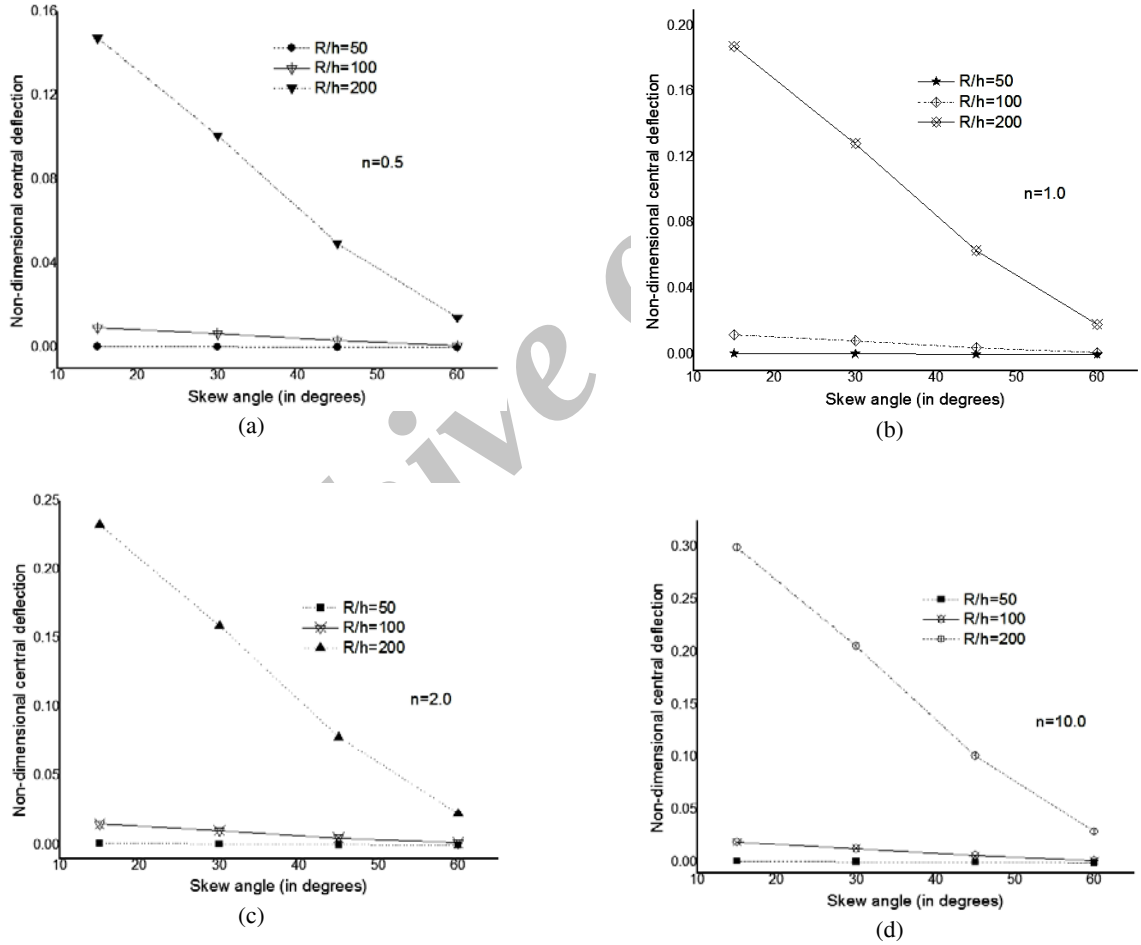

Fig. 4
Influence of radius (R_x) on deflection for cylindrical skew shell (type II FGM, mechanical load).

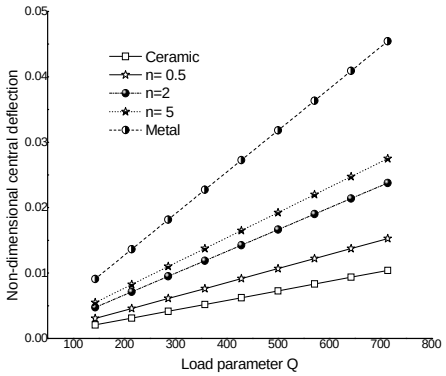

Fig. 5
Influence of Load parameter on deflection for cylindrical skew shell (type II FGM, mechanical load).

6 CONCLUSIONS

Bending analysis of different types of functionally graded skew shells with various geometries namely cylindrical, spherical, hyperbolic paraboloid and hyper has been carried out using a nine noded C_0 isoparametric Lagrangian element with seven nodal unknowns per each node, for the first time. The Voigt rule of mixture is used to estimate the effective elastic properties of the FGM shell. The displacement field is expressed based on a higher order shear deformation theory (HSDT) which requires no shear correction factor unlike first order shear deformation theory (FSDT) and Sander's approximation is used to represent the linear strain components. The response of the different types of skew shells under mechanical and thermal field is studied by performing various numerical examples. Following vital comments are put forward regarding bending analysis of FGM skew shells.

- Increase in skew angle confirms less magnitude of deflection irrespective of the nature of boundary condition of the panel.
- Clamped skew shell ensures minimum deflection compared with SSSS and SCSC boundary conditions due to high rigidity phenomenon.
- Hypar skew shells shows better performance compared to spherical and hyperbolic paraboloid shells in view of deflection criteria.
- Temperature field will have noticeable consequence on deflection criteria of the panel. It tends to rise the deflection when it goes up.
- In all the examples performed, increase in volume fraction index *n* tends to record high deflection due to less stiffness offered by metal segment.
- On the whole, volume fraction index *n* and skew angle (*a*) of the shell are found to be a key parameter in predicting the bending response of the shell.

Further, the work of sandwich functionally graded plates considering the thickness stretching effect is under the study by authors.

APPENDIX A

$$\{\varepsilon\} = \sum_{i=1}^{9} \begin{bmatrix}
\frac{\partial N_i}{\partial x} & 0 & N_i R_x & 0 & 0 & 0 & 0 \\
0 & \frac{\partial N_i}{\partial y} & 0 & N_i R_y & 0 & 0 & 0 \\
\frac{\partial N_i}{\partial y} & \frac{\partial N_i}{\partial x} & 2N_i R_{xy} & 0 & 0 & 0 & 0 \\
-N_i C_1 R_x & -N_i C_1 R_{xy} & \frac{\partial N_i}{\partial x} & N_i & 0 & 0 & 0 \\
-N_i C_1 R_{xy} & -N_i C_1 R_y & \frac{\partial N_i}{\partial y} & 0 & N_i & 0 & 0 \\
0 & 0 & 0 & \frac{\partial N_i}{\partial x} & 0 & 0 & 0 \\
0 & 0 & 0 & 0 & 0 & \frac{\partial N_i}{\partial x} & 0 \\
0 & 0 & 0 & 0 & \frac{\partial N_i}{\partial y} & 0 & 0 \\
0 & 0 & 0 & 0 & 0 & 0 & \frac{\partial N_i}{\partial y} \\
0 & 0 & 0 & \frac{\partial N_i}{\partial y} & \frac{\partial N_i}{\partial x} & 0 & 0 \\
0 & 0 & 0 & 0 & 0 & \frac{\partial N_i}{\partial y} & \frac{\partial N_i}{\partial x} \\
0 & 0 & 0 & -N_i C_1 R_x & -N_i C_1 R_{xy} & 0 & 0 \\
0 & 0 & 0 & 0 & 0 & -N_i C_1 R_x & -N_i C_1 R_{xy} \\
0 & 0 & 0 & -N_i C_1 R_{xy} & -N_i C_1 R_y & 0 & 0 \\
0 & 0 & 0 & 0 & 0 & -N_i C_1 R_{xy} & -N_i C_1 R_y \\
0 & 0 & 0 & N_i & 0 & N_i & 0 \\
0 & 0 & 0 & 0 & N_i & 0 & N_i
\end{bmatrix} \tag{A.1}$$

REFERENCES

[1] Gasik M.M., 2010, Functionally graded materials: bulk processing techniques, *International Journal of Materials and Production Technology* **39**(1–2):20–29.

[2] Jha D.K., Tarun Kant R.K., Singh., 2013, A critical review of recent research on functionally graded plates, *Composite Structures* **96**: 833-849.

[3] Praveen G.N., Reddy J.N., 1998, Nonlinear transient thermoelastic analysis of functionally graded ceramic–metal plates, *International Journal of Solids and Structures* **35**:4457–4471.

[4] Reddy J.N., Wang C.M., Kitipornchai S., 1999, Axisymmetric bending of functionally graded circular and annular plates, *European Journal of Mechanics A/Solids* **18**:185–99.

[5] Reddy J.N., 2000, Analysis of functionally graded plates, *International Journal of Numerical Methods in Engineering* **47**:663–684.

[6] Vel S.S., Batra R.C., 2002, Exact solutions for thermoelastic deformations of functionally graded thick rectangular plates, *AIAA Journal* **40**(7):1421–33.

[7] Shen H.S., 2005, Postbuckling of FGM plates with piezoelectric actuators under thermo-electro-mechanical loadings, *International Journal of Solids and Structures* **42**:6101–6121.

[8] Tsukamoto H., 2003, Analytical method of inelastic thermal stresses in a functionally graded material plate by a combination of a micro and macromechanical approaches, *Composites Part B* **34**(6):561–8.

[9] Qian L.F., Batra R.C., Chen L.M., 2004, Analysis of cylindrical bending thermoelastic deformations of functionally graded plates by a meshless local Petrov– Galerkin method, *Computational Mechanics* **33**:263–73.

[10] Lanhe W., 2004, Thermal buckling of a simply supported moderately thick rectangular FGM plate, *Composite Structures* **64**:211–218.

[11] Ferreira A.J.M., Batra R.C., Roque C.M.C., Qian L.F., Martins P.A.L.S., 2005, Static analysis of functionally graded plates using third-order shear deformation theory and a meshless method, *Composite Structures* **69**:449–457.

[12] Zenkour A.M., 2007, Benchmark trigonometric and 3-D elasticity solutions for an exponentially graded thick rectangular plate, *Archive of Applied Mechanics* **77**:197–214.

[13] Kim Y.W., 2005, Temperature dependent vibration analysis of functionally graded rectangular plates, *Journal of Sound and Vibration* **284**:531–549.

[14] Javaheri R, Eslami M.R., 2003, Thermal buckling of functionally graded plates based on higher order theory, *Journal of Thermal Stresses* **25**:603–625.

[15] Na K.S., Kim J.H., 2004, Three-dimensional thermal buckling analysis of functionally graded materials, *Composites Part B* **35**:429–437.

[16] Neves A.M.A., Ferreira A.J.M., Carrera E, Roque C.M.C., Cinefra M, Jorge R.M.N., 2012, A quasi-3D sinusoidal shear deformation theory for the static and free vibration analysis of functionally graded plates, *Composites Part B* **43**:711–725.

[17] Naghdi P.M., 1956, A survey of recent progress in the theory of elastic shells, *Applied Mechanics Reviews* **9**: 365-368.

[18] Bert C.W., 1976, Dynamics of composite and sandwich panels-Part I, *Journal of Shock and Vibration* **8***:* 37-48.

[19] Bert C.W., 1980, *Analysis of Shells. Analysis and Performance of Composites*, Wiley, New York .

[20] Hildebrand F.B., Reissner E, Thomas G.B., 1949, Note on the foundations of the theory of small displacements of orthotropic shells, *Advisory Committee for Aeronautics Techical Notes, No. 1833.*

[21] Lure A.I., 1947, *Statics of Thin Elastic Shells ,* Gostekhizdat, Moscow .

[22] Reissner E., 1952, Stress-strain relations in the theory of thin elastic shells, *Journal of Mathematical Physics* **31**: 109-119.

[23] Whitney J.M., Sun C.T., 1973, A higher order theory for extensional motion of laminated anisotropic shells and plates, *Journal of Sound and Vibration* **30**: 85-89.

[24] Whitney J.M., Sun C.T., 1974, A refined theory for laminated anisotropic cylindrical shells, *Journal of Applied Mechanics* **41**(2):471-476.

[25] Reddy J.N., 1983, Exact solutions of moderately thick laminated shells, *Journal of Engineering Mechanics* **110** (5): 794-809.

[26] Reddy J.N., Arciniega R.A., 2004, Shear deformation plate and shell theories: From Stavsky to present, *Journal of Mechanics of Advanced Materials and Structures* **11**: 535-582.

[27] Ferreira A.J.M., Roque C.M.C., Carrera E., Cinefra M., Polit O, 2011, Two higher order zigzag theories for the accurate analysis of bending, vibration and buckling response of laminated plates by radial basis functions collocation and a unified formulation, *Journal of Composite Materials* **45**(24):2523–2536.

[28] Ferreira A.J.M, Roque C.M.C., Carrera E, Cinefra M, Polit O, 2011, Radial basis functions collocation and a unified formulation for bending, vibration and buckling analysis of laminated plates, according to a variation of murakami's zig-zag theory, *European Journal of Mechanics A/Solids* **30**(4):559–570.

[29] Carrera E., Brischetto S., Robaldo A., 2008, Variable kinematic model for the analysis of functionally graded material plates, *AIAA Journal* **46**:194–203.

[30] Carrera E., Brischetto S., Cinefra M., Soave M., 2011, Effects of thickness stretching in functionally graded plates and shells, *Composite Part B* **42**:23–133.

[31] Qian L.F., Batra R.C., Chen L.M., 2004, Analysis of Cylindrical Bending Thermoelastic Deformations of Functionally Graded Plates by a Meshless Local Petrov-Galerkin Method, *Computational Mechanics* **33**: 263–273.

[32] Pradyumna S., Namit Nanda, Bandyopadhyay J.N., 2010, Geometrically nonlinear analysis of functionally graded shell panels using a higher order finite element formulation, *Journal of Mechanical Engineering and Research* **2**(2): 39-51.

[33] Zhao X., Liew K.M., 2009, Geometrically nonlinear analysis of functionally graded shells, *Journal of Mechanical Sciences* **51**: 131-144.

[34] Zhao X., Lee Y., Liew K.M., 2009, Thermoelastic and vibration analysis of functionally graded cylindrical shells, *Journal of Mechanical Sciences* **51**: 694-707.

[35] Naghdabadi R., Hosseini Kordkheni, S.A., 2005, A finite element formulation for analysis of functionally graded plates and shells, *Archive of Applied Mechanics* **74**: 375-386.

[36] Cinefra M., Carrera E., Brischetto S., Belouettar S., 2010, Thermo-Mechanical analysis of functionally graded shells, *Journal of Thermal Stresses* **33**: 942-963.

[37] Najafizadeh M.M., Isvandzibaei M.R., 2007, Vibration of functionally graded cylindrical shells based on higher order shear deformation plate theory with ring support, *Acta Mechanica* **191**: 75-91.

[38] Najafizadeh M.M., Hasani A., Khazaeinejad P., 2009, Mechanical stability of functionally graded stiffened cylindrical shells, *Applied Mathematical Modelling* **33**: 1151-1157.

[39] Najafizadeh M.M., Isvandzibaei M.R., 2009, Vibration of functionally graded cylindrical shells based on different shear deformation shell theories with ring support under various boundary conditions, *Journal of Mechanical Science and Technology* **23**: 1-13.
[40] Khazaeinejad P., Najafizadeh M.M., 2010, Mechanical buckling of cylindrical shells with varying material properties, *Proceedings of the Institution of Mechanical Engineers, Part C, Journal of Mechanical Engineering Science* **224**(8): 1551-1557.
[41] Khazaeinejad P., Najafizadeh M.M., Jenabi J., Isvandzibaei M.R., 2010, On the buckling of functionally graded cylindrical shells under combined external pressure and axial compression, *ASME Journal of Pressure Vessel and Technology* **132**(6): 064501-1-6.
[42] Najafizadeh M.M., Khazaeinejad P., 2010, An analytical solution for buckling of non-homogeneous cylindrical shells under combined loading, *Journal of Applied Mechanics Research* **2***(2):11-20.*
[43] Woo S, Meguid, S.A., 2001, Non linear analysis of functionally graded plates and shallow shells, *Journal of Solids and Structures* **38**: 7409-7421.
[44] Liew K.M., Kitipornchai S., Zhang X.Z., Lim C.W., 2003, Analysis of the thermal stress behavior of functionally graded hollow circular cylinders, *International Journal of Solids and Structures* **40**: 2355-2380.
[45] Jacob L.P., Vel. S.S., 2006, An exact solution for the steady-state thermoelastic response of functionally graded orthotropic cylindrical shells, *International Journal of Solids and Structures* **43**: 1131-1158.
[46] Woo J., Meguid, S.A., Stranata, J.C, Liew, K.M., 2005, Thermomechanical post buckling analysis of moderately thick functionally graded plates and shallow shells, *International Journal of Mechanical Sciences* **47**: 1147-1171.
[47] Bahtui A., and Eslami M.R., 2007, Generalized coupled thermoelasticity of functionally graded cylindrical shells, *International Journal of Numerical Methods in Engineering* **69**: 676-697.
[48] Reddy J.N., 1984, A simple higher-order theory for laminated composite plate, *Journal of Applied Mechanics* **51**: 745-752.
[49] Hill R., 1965, A self-consistent mechanics of composite materials, *Journal of Mechanics and Physics of Solids* **13**:213–222.
[50] Hashin Z., 1968, Assessment of the self consistent scheme approximation: conductivity of composites, *Journal of Composite Materials* **4**:284–300.
[51] Bhaskar K., Varadan T.K, 2001, Assessment of the self consistent scheme approximation: conductivity of composites, *ASME Journal of Applied Mechanics* **68**(4):660–2.
[52] Mori T., Tanaka T., 1973, Average stress in matrix and average elastic energy of materials with misfitting inclusions, *Acta Metallaugica* **21**:571–574.
[53] Benveniste Y., 1987, A new approach to the application of Mori–Tanaka's theory in composite materials, *Mechanics of Materials* **6**:147–157.
[54] Hashin Z., 1962, The elastic moduli of heterogeneous materials, *ASME Journal of Applied Mechanics* **29**:143–150.
[55] Hashin Z., Shtrikman S., 1964, A variational approach to the theory of elastic behaviour of multiphase materials, *Journal of mechanics and physics of solids* **11**:127–140.
[56] Hashin Z., Rosen B.W., 1964, The elastic moduli of fiber-reinforced materials, *ASME Journal of Applied Mechanics* **4**:223–232.
[57] Hashin Z., 1979, Analysis of properties of fiber composites with anisotropic constituents, *ASME Journal of Applied Mechanics* **46**:543–450.
[58] Chamis C.C., Sendeckyj G.P., 1968, Critique on theories predicting thermoelastic properties of fibrous composites, *Journal of Composite Materials* **2**(3):332–358.
[59] Gibson R.F., 1991, *Principles of composite material mechanics*, McGraw-Hill.
[60] Aboudi J., 1991, *Mechanics of composite materials: a unified micromechanical approach,* Amsterdam, Elsevier.
[61] Suresh S., Mortensen A., 1998, *Fundamentals of Functionally Graded Material,* London, IOM Communications.